Cationic and Anionic Vacancies in the Crystalline Phases of Sol−Gel Magnesia−Alumina Catalysts

J. A. Wang, A. Morales, X. Bokhimi,* and O. Novaro†

Institute of Physics, The National University of Mexico (UNAM), A. P. 20-364, 01000 Mexico D.F., Mexico

T. López and R. Gómez

Department of Chemistry, Universidad Autónoma Metropolitana-Iztapalapa, A. P. 55-534, 09340 Mexico D.F., Mexico

Received July 31, 1998. Revised Manuscript Received November 11, 1998

Magnesium−alumina mixed oxide catalysts at Mg:Al atomic ratios of 3:1, 2:1.8, and 1:2.8 were synthesized by using the sol−gel technique. Dehydroxylation and phase transformations were studied with thermogravimetry. Crystalline structures were measured with X-ray powder diffraction. Position and concentration of anionic and cationic vacancies were obtained by refining crystalline structures with the Rietveld technique. When samples were annealed below 400 °C, boehmite, brucite, hydrotalcite, and glushinskite were formed. When they calcined at 600 °C, boehmite was transformed into γ-Al_2O_3, and brucite, hydrotalcite, and glushinskite into periclase. In magnesium-rich samples, magnesium ions were incorporated into the γ-Al_2O_3 lattice, expanding its unit cell. Sample dehydroxylation produced oxygen vacancies in boehmite, brucite, and θ-Al_2O_3. Periclase and γ-Al_2O_3, however, had cationic vacancies in concentrations that depended on calcining temperature. Different models are proposed for explaining the formation mechanisms of the anionic and cationic vacancies.

1. Introduction

In solid catalysts, defects in the crystalline structures, including both cationic and anionic vacancies, can act as active reaction centers. The study of these defects would help to understand some catalytic reaction mechanisms; their quantification, however, is difficult.

Recent studies of catalysts with X-ray powder diffraction and crystalline structure refinement have proved that these techniques are powerful tools for the identification of defects in lattices.[1−6] They are especially effective to characterize nanocrystalline materials.

The generation of defects in crystalline structures is usually related to the synthesis methods. For example, in sol−gel titania calcined between 70 and 900 °C, titanium vacancies are found in the three crystalline phases, brookite, anatase, and rutile.[2] In sol−gel alumina, oxygen vacancies are found in its precursor, boehmite, and aluminum vacancies in γ-Al_2O_3.[6] Similarly, vacancies are found in sol−gel magnesia: oxygen vacancies in its precursor, brucite, and magnesium vacancies in periclase.[1,3] Ammonia and CO_2 adsorption on sol−gel MgO show that magnesia defects give rise to acidic and basic sites.[3]

Crystalline structure defects in catalysts affect their catalytic properties. For example, the defects in sol−gel alumina and sol−gel magnesia catalysts catalyze 2-propanol decomposition.[4,7] In sol−gel alumina, cationic and oxygen vacancies are directly involved in the formation of acetone and isopropyl ether during 2-propanol decomposition.[4,5]

In the present work, we are interested in studying magnesia−alumina mixed oxides as catalytic materials. In this system, the intermediate compound hydrotalcite ($Mg_6Al_2(OH)_xA_n.mH_2O$) is formed when samples are calcined at low temperatures. This compound is transformed into spinel ($MgAl_2O_4$) when annealing temperature is increased.[8−14]

* To whom correspondence should be addressed. Tel. (525) 622-5079. Fax. (525) 622-5008. E-mail: bokhimi@fenix.ifisicacu.unam.mx.

† Member of El Colegio Nacional, Mexico.

(1) Portillo, R.; López, T.; Gómez, R.; Bokhimi, X.; Morales, A.; Novaro, O. *Langmuir* **1996**, *12*, 40.

(2) Bokhimi; Morales, A.; Novaro, O.; López, T.; Sánchez, E.; Gómez, R. *J. Mater. Res.* **1995**, *10*, 2788.

(3) Wang, J. A.; Novaro, O.; Bokhimi, X.; López, T.; Gómez, R.; Navarrete, J.; Llanos, M. E.; López-Salinas, E. *J. Phys. Chem.* **1997**, *101*, 7448.

(4) Wang, J. A.; Novaro, O.; Bokhimi, X.; López, T., Gómez, R., Navarrete, J., Llanos, M.; López-Salinas E. *J. Mol. Catal.* **1998**, *137*, 239.

(5) Wang, J. A.; Novaro, O.; Bokhimi, X.; López, T.; Gómez, R. Cancun '97 International Materials Research Congress, S12−15, Sept 1−4, 1997, Cancún, Mexico.

(6) Wang, J. A.; Bokhimi, X., Morales, A.; Novaro, O.; López, T.; Gómez, R., *J. Phys. Chem.* Submitted, 1998.

(7) Wang, J. A.; Bokhimi, X.; Novaro, O.; López, T.; Gómez, R. *J. Mol. Catal.* Submitted, 1998.

(8) Carrado, K. A.; Kostapapas, A. *Solid State Ionics* **1988**, *26*, 78.

(9) Dimotakis, E. D.; Pinnavaia, T. J. *Inorg. Chem.* **1990**, *29*, 2393.

(10) Corma, A.; Fornes, V.; Martin-Aranda, R. M.; Rey, F. *J. Catal.* **1992**, 134, 58.

(11) Miya, S. *Clays Clay Miner.* **1985**, *28*, 370.

(12) Valcheva-Traykova, M. L.; Davidova, N. P.; Weiss, A. H. *J. Mater. Sci.* **1993**, *28* 2157.

(13) López, T.; Bosch, P.; Ramos, E.; Gómez, R.; Novaro, O.; Acosta, D.; Figueras, F. *Langmuir* **1996**, *12*, 189.

(14) Kazansky, V. B.; Borovkov, V. Yu.; Serykh, A. I.; Figueras, F. *Catal. Lett.* **1997**, *49*, 35.

10.1021/cm9805471 CCC: $18.00
Published on Web 01/20/1999

Samples were prepared with the sol−gel method, which produced magnesia−alumina catalysts with very fine particles, large specific surface areas, and lattice defects. Since sol−gel magnesia and sol−gel γ-alumina have magnesium and aluminum vacancies, respectively,[1,3,5,15,16] by diffusing through the oxygen framework, magnesium ions could occupy cation vacancies in γ-alumina. Similarly, aluminum ions can also occupy the magnesium vacancies in magnesia. Hence, the structural rearrangements and lattice distortions in the crystalline structures of the above crystalline phases will give rise to important effects on their catalytic properties.

The formation mechanism of the above structural vacancies is not clear. Therefore, we used X-ray powder diffraction and refined the crystalline structure of the phases in the samples to determine the concentrations, types, and positions of the vacancies in the crystalline structures. Several models are proposed to explain the formation mechanisms.

2. Experimental Section

2.1. Sample Preparation. Magnesium ethoxide (Aldrich, 99%), dissolved in buthanol, was mixed with the hydrolysis catalyst oxalic acid (Baker, 99%) to give pH 5. This solution was refluxed and stirred for 3 h at 70 °C. Afterward, aluminum tri-sec-butoxide and water were slowly dropped into the solution until the gel formed, which was dried at 70 °C (fresh sample). Before characterization, fresh samples were calcined in air at 200, 400, 600, or 800 °C for 4 h.

Besides pure magnesia and pure alumina, samples with Mg:Al atom ratios of 3:1 (MGAL31), 2:1.8 (MGAL22), and 1:2.8 (MGAL13) were prepared.

2.2. Thermogravimetric Analysis. Thermogravimetric (TG) analysis was carried out under flowing N_2 in a DuPont 2100 thermoanalyzer apparatus. About 20 mg of sample was placed in a quartz pan and heated from room temperature to 800 °C at 10 °C/min.

2.3. X-ray Diffraction Analysis and Rietveld Refinement. X-ray powder diffraction was performed at room temperature with a Siemens D-5000 diffractometer having Cu Kα radiation. Intensities were measured at 2θ diffraction angles between 8° and 110°, with 0.02° step size and 2.67 s measuring time per point. DBWS-9600PC[17] and WYRIET[18] codes were used to refine crystalline structures with the Rietveld method. Standard deviations, showing the variation of the last figures of the corresponding numbers, are given in parentheses. When they correspond to parameters obtained from the Rietveld refinement, the reported values are not estimates of the probable error in the analysis as a whole but only of minimum possible probable errors based on normal distribution.[19]

3. Results

3.1. Thermogravimetric Analysis. The TG curve of MGAL31 samples had three weight loss stages (Figure 1). The first (0.6% of weight loss) and second stages (4.7% of weight loss) appeared between 25 and 128 °C and were produced by the evaporation of residual water and solvents. A remarkable DTG (the derivative of the TG curve) peak in the third stage, which occurred between 244 and 601 °C and was centered at 355 °C,

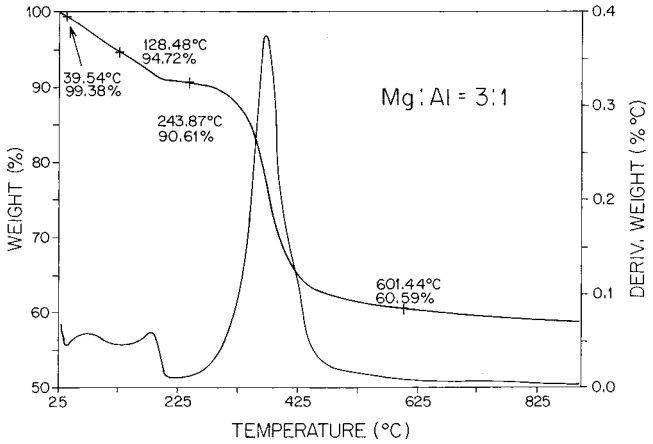

Figure 1. Thermogravimetric analysis of MGAL31 samples.

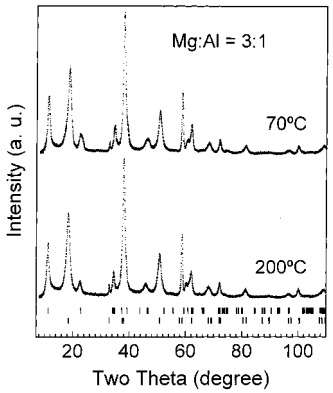

Figure 2. X-ray diffraction patterns of the MGAL31 samples calcined at 70 and 200 °C. The upper set of tick marks corresponds to hydrotalcite and the lower set to brucite.

corresponded to a weight loss of 30%. In pure magnesia, a similar peak, centered at 325 °C in the TG curve, was ascribed to brucite dehydroxylation.[20] In 100% alumina, a similar peak was also observed at 375 °C, produced by boehmite dehydroxylation.[6]

MGAL31 samples calcined below 200 °C contained brucite and hydrotalcite but not boehmite (Figure 2).

The weight loss of 30% was related to the dehydroxylation and decomposition of brucite and hydrotalcite (mainly to brucite, the main phase).

MGAL22 and MGAL13 samples, calcined below 200 °C, also had the two weight losses (Figures 3 and 4) ascribed to the evaporation of the residual water and solvent. When these samples were annealed above 200 °C, two more weight-loss stages were observed. The intensity of the stage between 400 and 600 °C increased when aluminum content increased, but it decreased for the one between 250 and 400 °C. This behavior was correlated to brucite and boehmite concentrations (Table 1).

Above 600 °C, sample weight variation with temperature was nearly zero, because brucite and boehmite decomposition was almost complete.

3.2. Phase Transformations. The MGAL31 samples dried at 70 °C contained brucite and hydrotalcite (Figure 2) and a small amount of glushinskite ($MgC_2O_4 \cdot H_2O$) produced by the presence of $C_2O_4^{2-}$ groups from the hydrolysis catalyst, oxalic acid. When they were calcined

(15) Well, A. F. *Structural Inorganic Chemistry*; Oxford Press: London, 1962.
(16) Soled, S. *J. Catal.* **1983**, *81*, 257.
(17) R. A. Young, R. A.; Sakthivel, A.; Moss, T. S.; Paiva-Santos, C. O. *J. Appl. Crystallogr.* **1995**, *28*, 366.
(18) Margarita Schneider EDV−Vertrieb Starnbergweg 18, D.-8134 Pöcking Germany, 1992. Tel. 0049-8157, Fax. 0048-8157 4527.
(19) Prince, E. *J. Appl. Crystallogr.* **1981**, *14*, 157.
(20) Zhou R. S.; Snyder, R. L. *Acta Crystallogr. B* **1991**, *47*, 617.

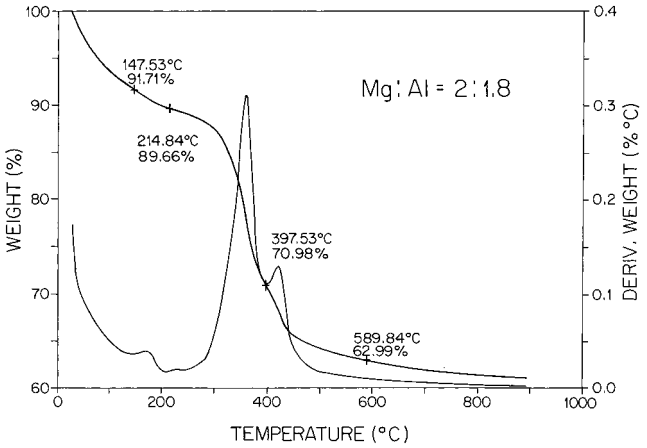

Figure 3. Thermogravimetric analysis of MGAL22 samples.

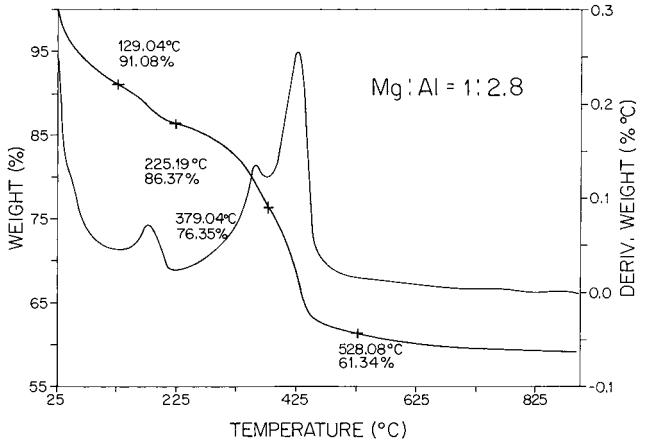

Figure 4. Thermogravimetric analysis of MGAAL13 samples.

Table 1. Phase Concentrations, in wt %, When Samples Were Calcined at 400 °C

samples	periclase	boehmite	hydrotalcite	γ-alumina
MGAL31	14.1(2)		19.0(4)	67(4)
MGAL22	4.0(2)	22(2)	9.3(3)	65(3)
MGAL13	3.0(8)	48(2)	7.2(2)	42(3)

at 200 °C, the only temperature effect was to evaporate absorbed water and solvents and to increase the average crystallite sizes.

When MGAL31 samples were annealed at 400 °C, several crystalline transformations were observed (Figure 5 and Table 1). Brucite was transformed into periclase; glushinskite was transformed into MgO, CO_2, and CO; and hydrotalcite was partially dehydroxylated. At this temperature, brucite and glushinskite totally disappeared, but not hydrotalcite; γ-alumina was generated.

When samples were calcined at 600 and 800 °C, they contained periclase and γ- and θ-alumina (Tables 2 and 3).

The MGAL22 and MGAL13 samples dried at 70 and calcined at 200 °C had brucite, glushinskite, hydrotalcite, and boehmite phases (Figures 6 and 7). The high aluminum content favored the formation of boehmite. When they were calcined at 400 °C, brucite and glushinskite disappeared, while boehmite and hydrotalcite concentrations were reduced (Table 1). The samples annealed at 600 or 800 °C did not contain boehmite any more. The diffraction peaks of periclase and alumina

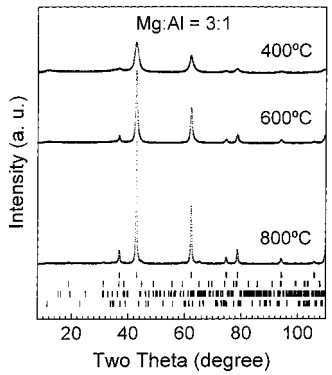

Figure 5. X-ray diffraction patterns of MGAL31 samples calcined at different temperatures. The first (upper) set of tick marks corresponds to periclase, the second set to γ-alumina, the third set to θ-alumina, and the lowest set to hydrotalcite.

Table 2. Phase Concentrations, in wt %, When Samples Were Calcined at 600 °C

samples	periclase	hydrotalcite	γ-alumina	θ-alumina
MGAL31	12.2(1)	15.4(9)	31(1)	41(3)
MGAL22	6.0(1)	11.9(1)	32(3)	50(2)
MGAL13	3.2(1)	2.1(2)	66(3)	29(8)

Table 3. Phase Concentrations, in wt %, When Samples Were Calcined at 800 °C

samples	periclase	hydrotalcite	γ-alumina	θ-alumina
MGAL31	15.7(4)	15.0(4)	37(1)	32(1)
MGAL22	4.6(9)	20.6(5)	35.9(5)	39(1)
MGAL13	6.1(2)	4.9(5)	43(4)	46(6)

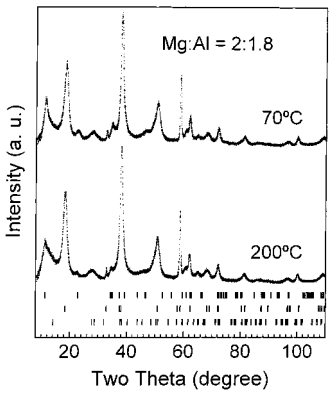

Figure 6. X-ray diffraction patterns of the MGAL22 samples calcined at 70 and 200 °C. The upper set of tick marks corresponds to hydrotalcite, the middle set to brucite, and the lower set to boehmite.

phases (γ- and θ-alumina) became narrow, indicating an increase of crystalline sizes (Figures 8 and 9).

3.3. Anionic and Cationic Vacancies in Crystalline Structures. In this section, we will focus on the study of vacancies in boehmite, alumina, and periclase, i.e., their positions in the unit cell, their types, and their concentrations.

The boehmite crystalline structure in MGAL22 and MGAL13 samples had oxygen vacancies. For example, there were 5 vacancies per unit cell in MGAL13 samples: 2.5 in the hydroxyl layer and 2.5 in the interlayer. The brucite in these samples was also oxygen deficient.

All samples calcined at 400, 600, or 800 °C contained γ-alumina with aluminum vacancies in both octahedral and tetrahedral aluminum sites (Tables 4−6).

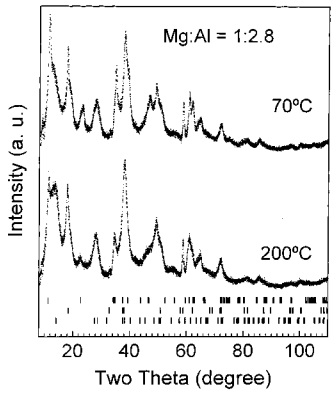

Figure 7. X-ray diffraction patterns of the MGAL13 samples calcined at 70 and 200 °C. The upper set of tick marks corresponds to hydrotalcite, the middle set to brucite, and the lower set to boehmite.

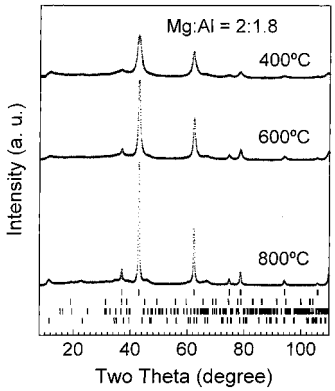

Figure 8. X-ray diffraction patterns of MGAL22 samples calcined at different temperatures. The first (upper) set of tick marks corresponds to periclase, the second set to γ-alumina, the third set to θ-alumina, and the lowest set to hydrotalcite.

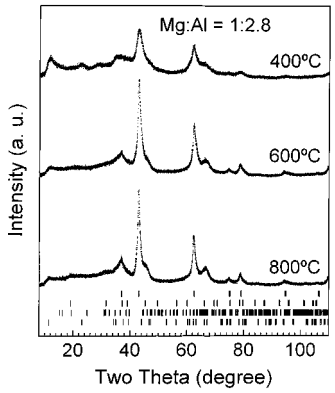

Figure 9. X-ray diffraction patterns of MGAL13 samples calcined at different temperatures. The first (upper) set of tick marks corresponds to periclase, the second set to γ-alumina, the third set to θ-alumina, and the lowest set to hydrotalcite.

Periclase was magnesium deficient (Table 7), with fewer Mg vacancies per unit cell than Al vacancies in γ-alumina, indicating a preference to the formation of aluminum defects.

4. Discussion

4.1. Dependence of Crystalline Structures on Mg:Al Atomic Ratio. Magnesium was incorporated into the γ-Al_2O_3 lattice. This is evident by comparing the X-ray diffraction patterns of the samples calcined at 800 °C (Figure 10). The intensity of the (400) and (440) diffraction peaks of γ-Al_2O_3 increased as aluminum content increased. Their positions shifted to larger diffraction angles, indicating that γ-Al_2O_3 had magne-

Table 4. Aluminum Atom Occupancy and Vacancy Concentrations of γ-Al_2O_3 in the Samples Calcined 400 °C

	aluminum occupancy		aluminum vacancy[a]			
samples	tetrahedral	octahedral	N_1	N_2	N_T	N_t
MGAL31	0.015(1)	0.052(2)	5.2	6.0	11.2	8.5
MGAL22	0.016(1)	0.052(2)	4.9	6.1	11.0	8.3
MGAL13	0.015(1)	0.064(4)	5.1	3.7	8.8	6.1

[a] N_1, number of aluminum vacancies per unit cell in tetrahedral position; N_2, number of aluminum vacancies per unit cell in octahedral position; N_T, total number of aluminum vacancies per unit cell; $N_t = N_T - 2.7$ and is related to the hydroxyls in lattice.

Table 5. Aluminum Atom Occupancy and Vacancy Concentrations of γ-Al_2O_3 in the Samples Calcined 600 °C

	aluminum occupancy		aluminum vacancy[a]			
samples	tetrahedral	octahedral	N_1	N_2	N_T	N_t
MGAL31	0.029(1)	0.055(2)	2.4	5.5	7.9	5.2
MGAL22	0.023(2)	0.069(5)	3.6	2.7	6.3	3.3
MGAL13	0.031(1)	0.060(3)	2.0	4.5	6.5	3.8

[a] N_1, number of aluminum vacancies per unit cell in tetrahedral position; N_2, number of aluminum vacancies per unit cell in octahedral position; N_T, total number of aluminum vacancies per unit cell; $N_t = N_T - 2.7$ and is related to the hydroxyls in lattice.

Table 6. Aluminum Atom Occupancy and Vacancy Concentrations of γ-Al_2O_3 in the Samples Calcined 800 °C

	aluminum occupancy		aluminum vacancy[a]			
samples	tetrahedral	octahedral	N_1	N_2	N_T	N_t
MGAL22	0.030(2)	0.071(4)	2.2	2.4	4.6	1.9
MGAL13	0.033(1)	0.072(4)	1.7	2.2	3.9	1.2

[a] N_1, number of aluminum vacancies per unit cell in tetrahedral position; N_2, number of aluminum vacancies per unit cell in octahedral position; N_T, total number of aluminum vacancies per unit cell; $N_t = N_T - 2.7$ and is related to the hydroxyls in lattice.

Table 7. γ-Al_2O_3 Unit Cell Expansion When Samples Were Calcined at 800 °C

samples	atomic ratio (Mg:Al)	lattice parameter a (nm)	$\Delta = a - a_1$[a] (nm)	Δ/a (%)
MGAL31	3:1	0.8093(3)	0.01929	2.44
MGAL22	2:1.8	0.7979(3)	0.00787	0.99
MGAL13	1:2.8	0.7976(2)	0.00758	0.96

[a] a_1 is the cell parameter of pure γ-Al_2O_3, 0.790 nm.

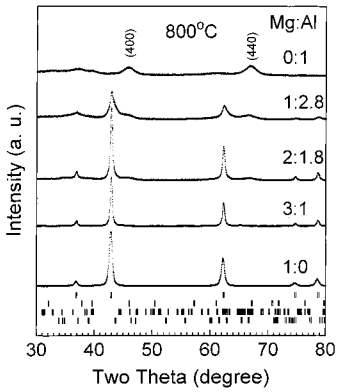

Figure 10. X-ray diffraction patterns of samples, calcined at 800 °C, with different Mg:Al atomic ratios. The first (upper) set of tick marks corresponds to periclase, the second set to γ-alumina, the third set to θ-alumina, and the lowest set to hydrotalcite.

sium in its crystalline structure. The γ-Al_2O_3 lattice parameter in MGAL31 samples was 0.8093(3) nm, compared to 0.7900 nm for pure γ-Al_2O_3.

Since γ-Al_2O_3 has the spinel ($MgAl_2O_4$) structure, Mg ions can occupy some of the tetrahedral sites in the structure to diminish the original cation deficiency (model 1; see Chart 1) and to stabilize the structure.

Chart 1. Model 1: Extra Magnesium Ion Occupies the Aluminum Defect (□) in the γ-Al_2O_3 Structure, Expanding the Unit Cell

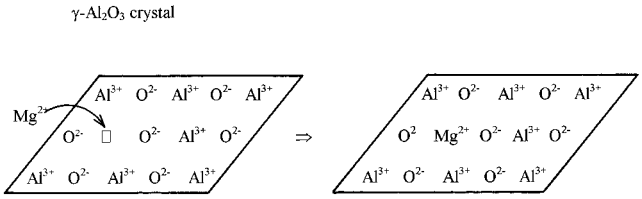

Since the magnesium ionic radius (0.071 nm) is larger than the aluminum ionic radius (0.067 nm), the incorporation of magnesium expanded the lattice.

The Mg:Al atomic ratio also affected the average crystalline size of the different phases: when aluminum content increased, the diffraction peaks became wider.

4.2. Mechanisms To Describe Oxygen Vacancies Origin. Brucite and boehmite had oxygen vacancies in their lattices. When samples were calcined above 600 °C, brucite completely transformed into periclase, and boehmite into γ-Al_2O_3; oxygen vacancies disappeared. The generation of these vacancies, therefore, was closely related to sample dehydroxylation and phase transformations.

When annealing temperature exceeded 400 °C, boehmite decomposed into γ-alumina. Hydroxyls left the boehmite lattice, and oxygen atoms rearranged, changing their hexagonal arrangement into a cubic one to generate γ-alumina. Adjacent hydroxyl layers interacted to produce water molecules, which were released through the irregular tunnels, leaving an unstable structure with oxygen vacancies. Since brucite has a lattice like boehmite, oxygen vacancies were also created in its structure during thermal treatment.

The lattice of the θ-Al_2O_3 produced when samples were calcined at 800 °C also had oxygen vacancies. Zhou and Snyder[20] report that some of the oxygen sites in this crystalline structure are not occupied. Hydroxyls are retained in the lattice, even in the samples calcined at 800 °C.[6,21] During the thermal treatment, especially at the highest calcining temperature, the retained OH groups escape from their positions, producing water molecules and oxygen vacancies (model 2; see Chart 2).

Chart 2. Model 2: Desorption of the Molecular Water Produced by the Reaction between the Hydroxyls in the MgO Lattice Creates Some Oxygen Defects (●)

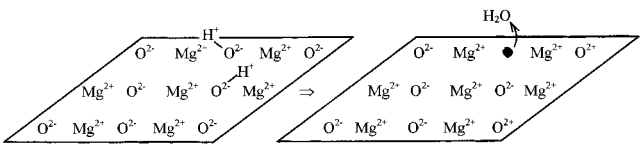

This mechanism differs from the one that explains the origin of oxygen vacancies in boehmite and brucite.

Table 8. Mg:O Atomic Ratio[a] of the Periclase in the Samples Calcined at Different Temperatures

sample	400 °C	600 °C	800 °C
MGAL31	0.949(5)	0.966(4)	0.991(2)
MGAL22	0.949(8)	0.950(2)	0.959(5)
MGAL13		0.936(1)	0.973(6)

[a] The ideal Mg:O atomic ratio of periclase is 1:1.

Summarizing, in sol−gel magnesium−alumina mixed oxides, generation of oxygen vacancies was closely related to the thermal treatment and transformation of the crystalline structures. Generation of oxygen vacancies was mainly determined by the reaction between retained hydroxyls in the lattice.

4.3. Mechanisms To Describe Cation Vacancies Origin. γ-Al_2O_3 and MgO lattices had aluminum and magnesium vacancies, respectively (Tables 3−6 and Table 8). During the partial transformation of brucite into periclase, some hydroxyls substituted for oxygen ions. This produced an extra positive charge that was compensated for with cation vacancies.[16]

The generation of aluminum vacancies in γ-Al_2O_3 depends on aluminum valence and the hydroxyls in the lattice. γ-Al_2O_3 has a spinel crystalline structure that has $A_8B_{16}C_{32}$ sites per unit cell available. A sites are normally occupied by ions with valence 2+ and are at the center of the tetrahedron formed by C sites, which for oxides is occupied by oxygen ions. B sites are normally occupied by ions with valence 3+ and are at the center of the octahedra formed by C sites. In γ-Al_2O_3, however, aluminum ions are all trivalent; therefore, to keep charge balance, 2.7 of the total A + B sites per unit cell must be empty.[22−25]

As discussed above, hydroxyls in the crystalline structure of oxides produce unbalanced local charge; to maintain the electrical neutrality, some cationic defects must be yielded. For example, in γ-Al_2O_3, their FTIR spectra show that even if samples are calcined at 800 °C, some absorption bands associated with hydroxyls are observed.[20] These hydroxyls in its structure produce extra aluminum vacancies.

In periclase and γ-Al_2O_3, the concentration of cationic vacancies decreased when the annealing temperature increased (Tables 3−6 and Table 8). Cation occupancy in crystalline solids is strongly affected by the cation diffusion that is mainly determined by annealing temperature. For example, in MGAL31 samples, the Mg:O atomic ratio in periclase decreased from 0.949(5) to 0.966(4) and 0.991(2) when they were calcined at 400, 600, and 800 °C, respectively. In the γ-Al_2O_3 of MGAL22 samples, the total number of aluminum vacancies diminished from 11.0 at 400 °C to 6.3 at 600 °C and 4.6 at 800 °C. A similar behavior was observed in samples MGAL31 and MGAL13.

5. Conclusions

In sol−gel magnesium−alumina mixed oxide catalysts, the samples annealed below 400 °C had brucite

(21) López, T.; Marmolejo, R.; Asomoza, M.; Solis, S.; Gómez, R.; Wang, J. A.; Bokhimi, X.; Novaro, O.; Navarrete, J.; Llanos, M. E.; López, E. *Materials Lett.* **1997**, *32*, 325.
(22) Lippens, B. C.; Boer, J. H. *Acta Crystallogr.* **1964**, *17*, 1312.
(23) Ervin, G. *Acta Cryst.* **1964**, *5*, 103.
(24) Verwey, E. J. W. *J. Chem. Phys.* **1935**, *3*, 592.
(25) Saalfeld, H.; Mehrotra, B. *Ber. Deutsch. Keram. Ges.* **1965**, *42*, 161.

and hydrotalcite; those with low magnesium content additionally had boehmite. When they were calcined above 400 °C, they contained periclase, γ-Al_2O_3, and θ-Al_2O_3.

Magnesium was partially dissolved in γ-Al_2O_3. It substituted for aluminum, expanding the lattice.

Brucite, boehmite, and θ-Al_2O_3 were oxygen deficient. The generation of oxygen vacancies in θ-Al_2O_3 at 800 °C was related to the formation of molecular water produced by the reaction between retained hydroxyls in the lattice.

Periclase and γ-Al_2O_3 had cation vacancies. In γ-Al_2O_3, aluminum vacancies appeared in both the octahedral and tetrahedral positions; some of the vacancies were caused by hydroxyls in its crystalline structure.

Cation diffusion determined cation-vacancy concentration and distribution. In periclase and γ-Al_2O_3, this concentration decreased when sample annealing temperature was increased.

Acknowledgment. J. A. Wang would like to acknowledge the financial support from the CONACyT (Mexico) for his postdoctoral studies at the Institute of Physics, The National University of Mexico (UNAM). We would like to thank to Dr. V. Castaño for the facilities for the thermoanalysis and Mr. Manuel Aguilar for technical assistance.

CM9805471